Pacific Northwest
NATIONAL LABORATORY

PNNL-37044

Down-selection of Innovative Fusion Materials

November 2024

Osman El-Atwani
Skye Supakul
Ishtiaque Karim Robin
Eda Aydogan

U.S. DEPARTMENT OF ENERGY

Prepared for the U.S. Department of Energy
under Contract DE-AC05-76RL01830

DISCLAIMER

PACIFIC NORTHWEST NATIONAL LABORATORY
operated by
BATTELLE
for the
UNITED STATES DEPARTMENT OF ENERGY
under Contract DE-AC05-76RL01830

Printed in the United States of America

Available to DOE and DOE contractors from
the Office of Scientific and Technical Information,
P.O. Box 62, Oak Ridge, TN 37831-0062
www.osti.gov
ph: (865) 576-8401
fox: (865) 576-5728
email: reports@osti.gov

Available to the public from the National Technical Information Service
5301 Shawnee Rd., Alexandria, VA 22312
ph: (800) 553-NTIS (6847)
or (703) 605-6000
email: info@ntis.gov
Online ordering: http://www.ntis.gov

PNNL-37044

Down-selection of Innovative Fusion Materials

November 2024

Osman El-Atwani
Skye Supakul
Ishtiaque Karim Robin
Eda Aydogan

Prepared for
the U.S. Department of Energy
under Contract DE-AC05-76RL01830

Pacific Northwest National Laboratory
Richland, Washington 99354

Abstract

The goal of this proposal is to develop and fundamentally understand the microstructure of refractory multi-component alloys (MCA) as fusion-relevant plasma facing and structural materials, a step to down-select innovative fusion materials prior to the process of advancing their technology readiness level (TRL). Developing materials is paramount to enable fusion as energy source since no existing material is capable of coping with such extreme conditions. We will aim at understanding the role of chemistry and microstructure in these complex multi-component alloys systematically comparing their performance with pure tungsten materials in terms of mechanical properties and manufacturability. Such understanding will open opportunities to optimize MCAs for fusion applications and has a potential of attracting industry partnership.

Summary

Innovative multi-component alloys (MCA) will be down selected as plasma facing materials and structural materials for fusion power. The main goal of this proposal is to develop and fundamentally understand the microstructure of refractory MCAs as fusion-relevant materials, a step to down-select innovative fusion materials prior to the process of advancing their technology readiness level (TRL).

Acknowledgments

This research was supported by the Physical and Computational Science Directorate (PCSD), under the Laboratory Directed Research and Development (LDRD) Program at Pacific Northwest National Laboratory (PNNL). PNNL is a multi-program national laboratory operated for the U.S. Department of Energy (DOE) by Battelle Memorial Institute under Contract No. DE-AC05-76RL01830.

Acronyms and Abbreviations

MCA = Multi-Component Alloys
TRL = Technologically Readiness Level
FPP = Fusion Power Plants
PMI = Plasma Materials Interactions
FM&T = Fusion Materials and Technology
INFUSE = Innovation Network for Fusion Energy
Nanocrystalline = NC
ODTT = Order to Disorder Transition Temperature
DFT = Density Functional Theory
CMC = Canonical Monte Carlo
SEM = Scanning Electron Microscope
TEM = Transmission Electron Microscope
APT = Atom Probe Tomography
IVEM = Intermediate Voltage Electron Microscope
ANL = Argonne National Laboratory
SRIM = Stopping Range of Ions in Matter
SAD = Selected Area Diffraction
BF = Bright Field
PVD = Physical Vapor Deposition
LSEM = Large Strain Extrusion Machining
SPD = Severe Plastic Deformation
BF-TEM = Bright-Field Transmission Electron Microscope
TEM = Transmission Electron Microscope
VAM = Vacuum Arc-melted

Contents

Abstract ii
Summary iii
Acknowledgments iv
Acronyms and Abbreviations v
1.0 Introduction 2
2.0 Research Design and Methodology 3
2.1 CALPHAD 3
2.2 Down-selected Vanadium Based Alloys for Fusion 3
3.0 Dual Beam Ion Irradiation of Vanadium Based Alloys 4
3.1 In-situ Dual Beam Irradiation at 700°C Results on Nanocrystalline Thin Film Vanadium-Based Alloy 4
3.2 In-situ Dual Beam Irradiation at 700°C Results of Polycrystalline Severe Plastic Deformed (SPD) Vanadium Based Alloy 5
3.3 In-situ Dual Beam Irradiation at 700°C Results of Coarse-Grained Vacuum Arc Melted Vanadium-Based Alloy 6
4.0 Conclusion/ Summary 8
5.0 References 9

Figures

Figure 1: Plot of the total dose in dpa (blue curve), He^+ implantation (green curve), and Kr^+ implantation (red curve) experienced by the vanadium-based alloys. 4
Figure 2: Selected area diffraction (SAD) and bright-field (BF) TEM image of the pristine vanadium-based alloy thin film (a). SAD and BF-TEM image of the vanadium-based alloy thin film after heating to 700°C (b), as well as after dual beam ion irradiation with 1 MeV Kr^+ and 16 KeV He^+ to ~6 dpa (c). An underfocused BF-TEM image (d) highlights the presence of small He bubbles observed to be distributed throughout the entire film. 5
Figure 3: Selected area diffraction (SAD) and bright-field (BF) TEM image of the pristine SPD vanadium-based alloy (a). SAD and BF-TEM image of the thin film vanadium-based alloy after heating to 700°C (b), as well as after dual beam ion irradiation with 1 MeV Kr^+ and 16 KeV He^+ to ~5.5 dpa (c). An underfocused BF-TEM image (d) highlights the presence of He bubbles at the grain boundaries. 6
Figure 4: Selected area diffraction (SAD) and bright-field (BF) TEM image of the pristine VAM vanadium-based alloy (a). SAD and BF-TEM image of the vanadium-based alloy thin film after heating to 700°C (b), as well as after dual beam ion irradiation with 1 MeV Kr^+ and 16 KeV He^+ to ~5.5 dpa (c). An underfocused BF-TEM image (d) highlights the presence of some He bubbles throughout the grain, though difficult to distinguish with the damage present. 6

1.0 Introduction

Plasma facing and divertor materials in future fusion devices must tolerate extreme environments, represented by fast neutrons (~14 MeV which can generate 30-40 dpa/year), high particle (mainly helium) fluxes (10^{23}~10^{24} $m^{-2}s^{-1}$), thermal loads (5-20 MW/m^2) and transient thermal fluxes (e.g. edge localized modes, ELMs) of several GW/m^2.[1] These conditions create challenges in not only the testing and evaluation of materials, but even in the development of materials that withstand these environments[1, 2]. One of the most studied materials under extreme fusion environments is tungsten (W), a strong candidate due to its fusion-favorable characteristics, such as high melting point, good thermal conductivity, low sputtering yield and low tritium retention [3]. However, W suffers from severe microstructural changes caused by dislocations, dislocation loops, voids, bubbles, fuzz, or raft formation [4-8], under different irradiation environments (helium plasma, low energy helium, or heavy ions to simulate neutron damage). These microstructural changes trigger alterations in mechanical and physical properties that can potentially lead to the end of operation of a fusion device. In the quest for new materials that can withstand severe irradiation and mechanical extremes for advanced fusion applications, several routes have been suggested [1]. Refining the grain size to leverage a high density of interfaces, which act as defect sinks to mitigate irradiation damage and increase strength, is one route. However, this route can suffer from some drawbacks such as the thermal stability of the nanocrystalline (NC) grains (coarsening at the application temperature) [9]. Another route is to develop alloys with improved strength, defect annihilation and recombination [10] and enhanced thermal stability. In the last two decades, a novel set of alloys based on nearly equi-atomic compositions of several principal elements have been developed [11-13]. Vanadium-based refractory alloys have been recently developed in the context of high temperature applications, showing high melting temperature (above 2873 K) and superior mechanical properties at high temperatures compared to Ni-based superalloys or pure tungsten [14, 15]. Therefore, we propose to down-select and characterize manufactured multi-component alloys with particular compositions (considering manufacturability, stability, order to disorder transition temperature (ODTT), and radioactivity) for fusion power that include relevant fusion-acceptable elements and properties. Examples are the Vanadium-based alloys which are suggested by the fusion community as priority structural materials. We aim to compare their morphology and properties with baseline commercial W to gain a fundamental understanding of the role of chemistry and microstructure in the material's behavior that allows for the development of optimized materials. The goal is to deconvolute the effect of microstructure from that of chemistry and understand their role in improving the mechanical performance. These material aspects are critical for industrial partners whose aim is to select innovative but promising fusion materials for their fusion designs.

2.0 Research Design and Methodology

There are two critical and outstanding aspects of MCAs that need to be resolved before advancing the TRL of these materials: 1- Down-selection of MCAs with elements of low radioactivity and compositions that guarantee single phase materials with no intermetallics (which can lead to embrittlement of the materials) and 2- Manufacturability in bulk forms with homogeneous microstructure as predicted by theory. Controlling manufacturing is critical so that other crucial aspects of the performance of these MCAs under extreme fusion conditions can be investigated and a clear comparison to other bulk materials can be established. This project comprises a detailed characterization of innovative materials for fusion power that the PI owns. The material's selection was based on CALPHAD screening methodology:

2.1 CALPHAD

The CALPHAD method approximates the Gibbs free energy of the alloys with empirical functional forms that are usually fitted to experimental data. Commonly used a Redlich-Kister expansion [16] for the enthalpy of mixing to consider non-regular solutions. Different approximations to the entropy can be made although the most common one is the ideal gas formulation, which is one of the main approximations of the method. Phase constituents and phase stability diagrams are extracted via CALPHAD, as implemented in the ThermoCalc software (with TCHEA5 [17] and MOBHEA2 [18] databases). Compositions that provide a wide range of single-phase BCC microstructures are then further down selected.

2.2 Down-selected Vanadium Based Alloys for Fusion

From literature and phase diagrams, vanadium-based alloys were selected and are manufactured and processed by different means to achieve a range of grain sizes ranging from coarse grain to nanocrystalline to evaluate the radiation tolerance as a function of material's microstructure. Vacuum arc melting (VAM) was used to fabricate coarse grained specimens, which were also subjected to severe plastic deformation (SPD) via large strain extrusion machining (LSEM) to produce polycrystalline samples with sub-micron grain sizes. Finally, to achieve nanocrystalline specimens with sub-100nm grain sizes, physical vapor deposition (PVD) was performed. To evaluate their irradiation resistance, the VAM, SPD, and PVD specimens were subjected to simultaneous in-situ dual beam ion irradiation of 1 MeV Kr^{+} and 16 KeV He^{+} at elevated temperatures above 650°C at the intermediate voltage electron microscope (IVEM) facility at Argonne National Laboratory (ANL). The results and discussed in the next section.

3.0 Dual Beam Ion Irradiation of Vanadium Based Alloys

To evaluate the radiation tolerance of the down-selected material systems, selected systems – namely vanadium-based MCAs – were irradiated simultaneously by 1 MeV Kr^+ and 16 KeV He^+ at the intermediate voltage electron microscope (IVEM) facility at Argonne National Laboratory (ANL). To prepare for these experiments, the Stopping Range of Ions in Matter (SRIM) and the Kinchin-Pease model, quick damage calculations were performed to convert the fluence to the respective displacement-per-atom (dpa) and results can be observed in Figure 2. The results presented in this report begin by discussing results from nanocrystalline thin film specimen, followed by a polycrystalline specimen, and finally a coarse-grained specimen.

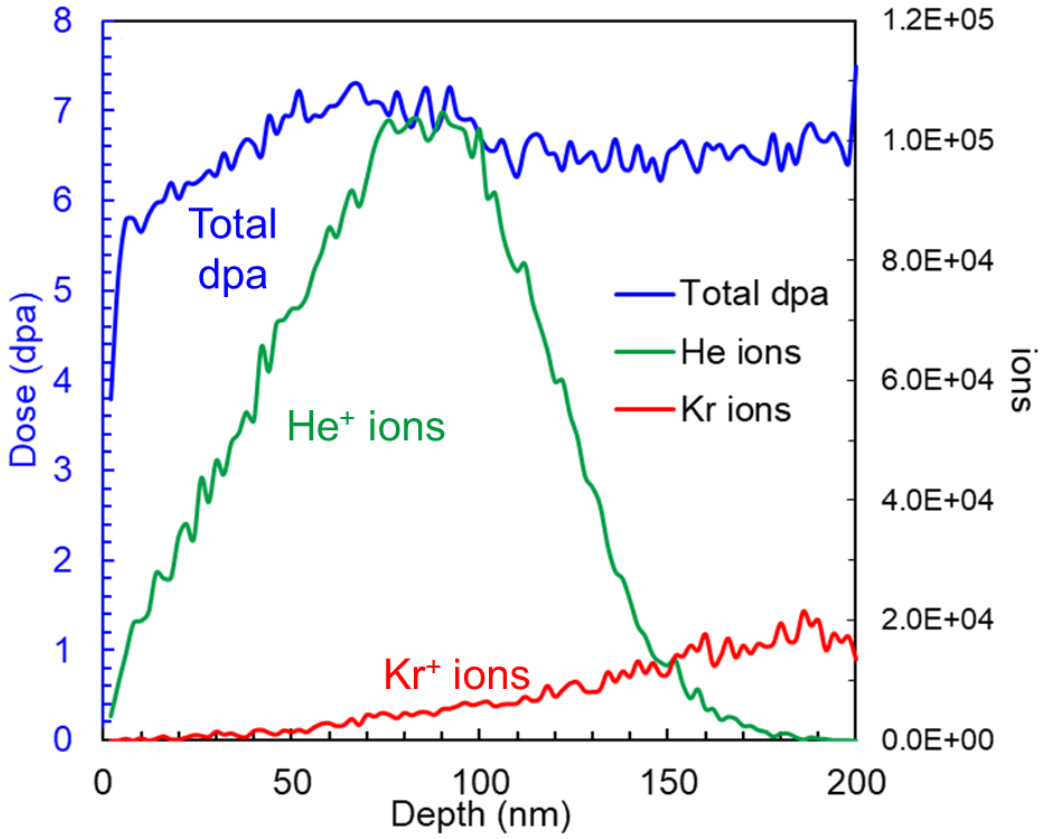

Figure 1: Plot of the total dose in dpa (blue curve), He^+ implantation (green curve), and Kr^+ implantation (red curve) experienced by the vanadium-based alloys.

3.1 In-situ Dual Beam Irradiation at 700°C Results on Nanocrystalline Thin Film Vanadium-Based Alloy

Bright-field (BF) TEM imaging with associated selected area diffraction (SAD) pattern of the pristine film prior to any exposure to temperature or irradiation can be observed in Figure 3a. From the diffraction pattern, the film is highly nanocrystalline, which is further supported by the BF-TEM image. The specimen was then heated in-situ to 700°C and the SAD and diffraction pattern upon reaching the target temperature of 700°C is shown in Figure 3b. Additional diffraction rings can be observed in the SAD (highlighted by the arrow), suggesting the formation of a possible secondary phase or precipitate due to the heating, however the grains remain

nanocrystalline as observed in the BF-TEM image. Finally, figure 3c shows the SAD and BF-TEM of the film after the dual beam ion irradiation to ~6 dpa. From the both the SAD and BF-TEM image, the film remains nanocrystalline, and the presence of the new secondary phase ring is still present. Figure 3d, is a BF-TEM image taken with an underfocus to highlight the presence of He bubbles. Small He bubble can be observe distributed throughout the entire film, suggesting a promising response to the elevated temperature dual beam ion irradiation to ~6 dpa.

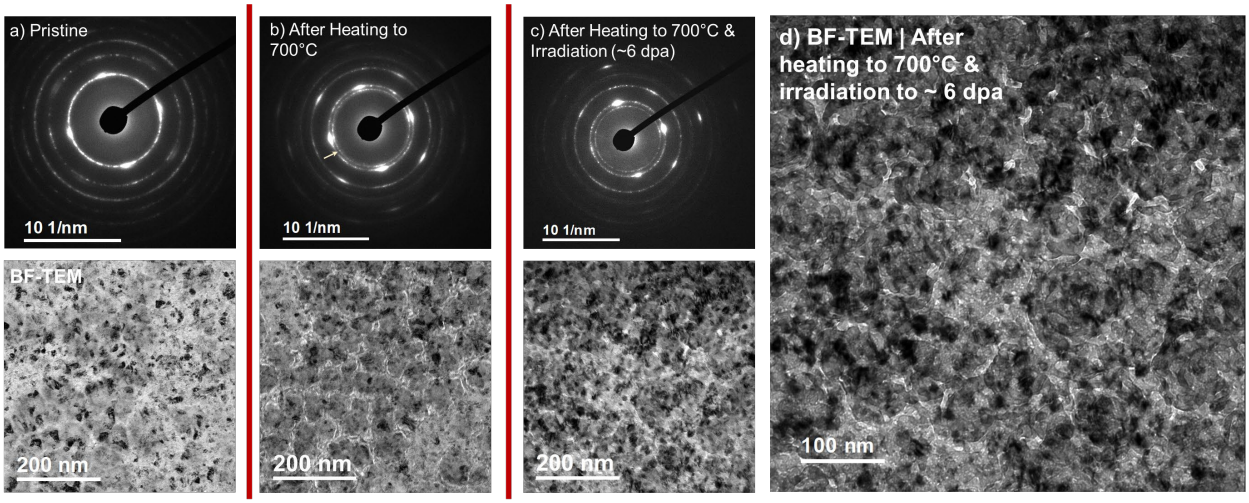

Figure 2: Selected area diffraction (SAD) and bright-field (BF) TEM image of the pristine vanadium-based alloy thin film (a). SAD and BF-TEM image of the vanadium-based alloy thin film after heating to 700°C (b), as well as after dual beam ion irradiation with 1 MeV Kr^{+} and 16 KeV He^{+} to ~6 dpa (c). An underfocused BF-TEM image (d) highlights the presence of small He bubbles observed to be distributed throughout the entire film.

3.2 In-situ Dual Beam Irradiation at 700°C Results of Polycrystalline Severe Plastic Deformed (SPD) Vanadium Based Alloy

Bright-field TEM imaging with associated selected area diffraction (SAD) pattern of the pristine SPD vanadium-based alloy prior to any exposure to temperature or irradiation can be observed in Figure 4a. From the diffraction pattern and the BF-TEM image, the sample polycrystalline with grains significantly larger than that observed in the previous nanocrystalline vanadium-based alloy thin film in section 3.1. The specimen was then heated in-situ to 700°C and the SAD and diffraction pattern upon reaching the target temperature of 700°C is shown in Figure 4b. There are a few diffraction spots which may indicate the presence of a secondary phase or precipitate, however further investigations would be required to confirm this. Similar to the thin film specimen, the grains exhibit negligible grain growth, and the grains are still in the polycrystalline regime. Figure 4c shows the SAD and BF-TEM of the SPD specimen after the dual beam ion irradiation to ~5.5 dpa. From the BF-TEM image, distinct dark contrast disc features can be observed throughout the film, likely to be carbide formations, common in vanadium-based alloys. Figure 4d, is a BF-TEM image taken with an underfocus to highlight the presence of He bubbles. Many He bubbles can be observed decorating the grain boundaries, and a few can be observed throughout the grains as well. Although the He bubbles remain small, their preferential formation at the grain boundaries may serve as weak spots for failure under mechanical load.

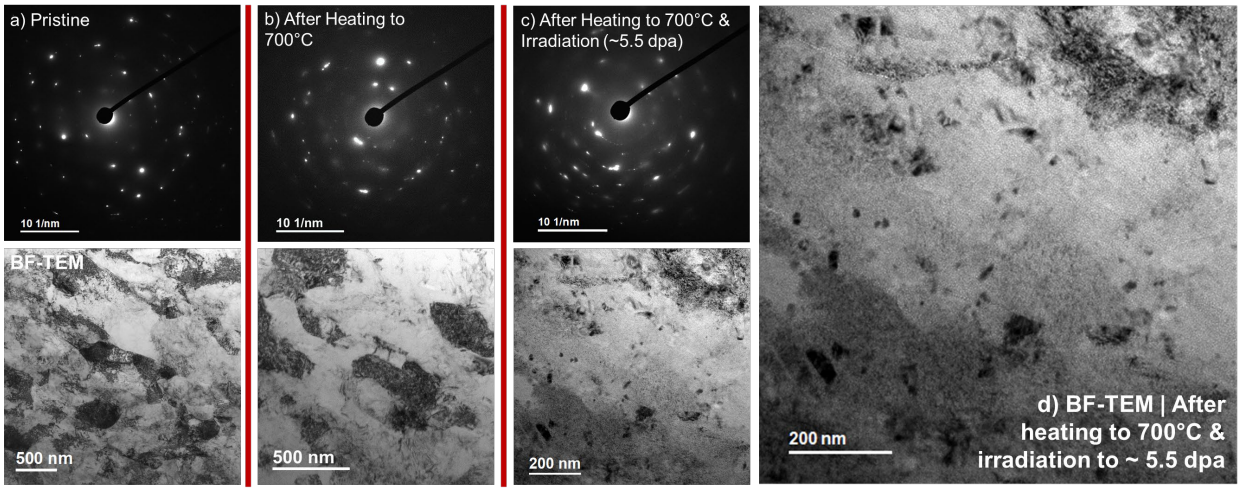

Figure 3: Selected area diffraction (SAD) and bright-field (BF) TEM image of the pristine SPD vanadium-based alloy (a). SAD and BF-TEM image of the thin film vanadium-based alloy after heating to 700°C (b), as well as after dual beam ion irradiation with 1 MeV Kr^+ and 16 KeV He^+ to ~5.5 dpa (c). An underfocused BF-TEM image (d) highlights the presence of He bubbles at the grain boundaries.

3.3 In-situ Dual Beam Irradiation at 700°C Results of Coarse-Grained Vacuum Arc Melted Vanadium-Based Alloy

Bright-field TEM imaging with associated selected area diffraction (SAD) pattern of the pristine vacuum arc melted (VAM) vanadium-based alloy prior to any exposure to temperature or irradiation can be observed in Figure 5a. From the diffraction pattern, the imaged region comes from a single grain, and dislocations can be observed throughout the region in the BF-TEM image. The specimen was then heated in-situ to 650°C and the SAD and diffraction pattern upon reaching

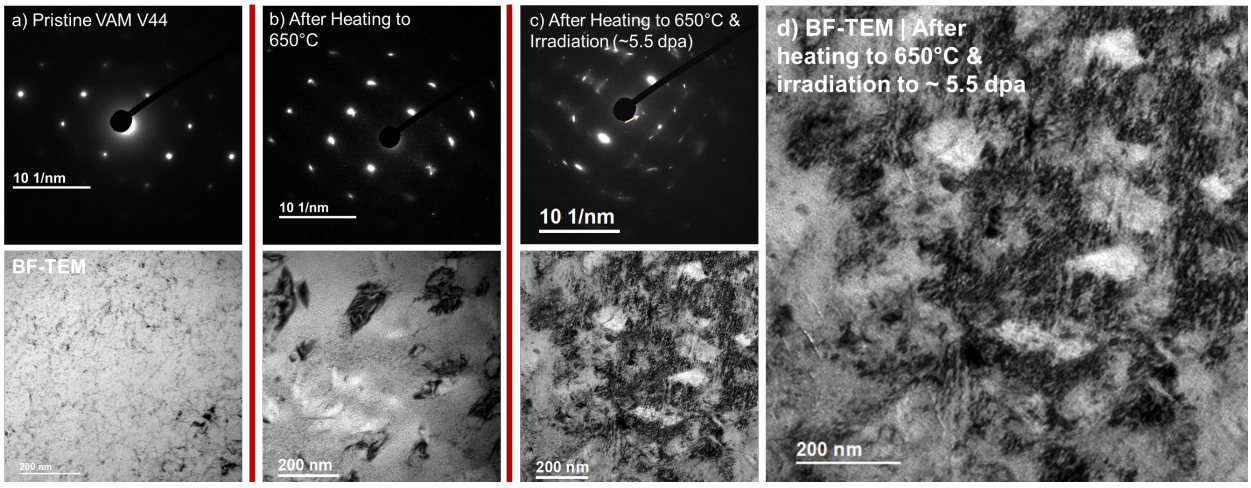

Figure 4: Selected area diffraction (SAD) and bright-field (BF) TEM image of the pristine VAM vanadium-based alloy (a). SAD and BF-TEM image of the vanadium-based alloy thin film after heating to 700°C (b), as well as after dual beam ion irradiation with 1 MeV Kr^+ and 16 KeV He^+ to ~5.5 dpa (c). An underfocused BF-TEM image (d) highlights the presence of some He bubbles throughout the grain, though difficult to distinguish with the damage present.

the target temperature of 650°C is shown in figure 5b. Heating for this specimen stopped at 650°C, which was the onset temperature for the formation of precipitates, as observed in the BF-TEM image. Figure 5c shows the SAD and BF-TEM of the VAM specimen after the dual beam ion irradiation to ~5.5 dpa. From the BF-TEM image, there is a lot more damage observed in the sample as compared to the previous two specimens as observed by the regions covered by dark contrast damage and defect features. The SAD also shows the presence of the other precipitates in the sample as highlighted by the arrow. Figure 5d, is a BF-TEM image taken with an underfocus to highlight the presence of He bubbles. Small He bubbles are observed sprinkled throughout the grain, however they are less distinguishable compared the SPD specimen in section 3.2. There may be the presence of more distinguishable He bubbles at the grain boundary, similar to the behavior observed in the SPD sample. Further investigation is required to confirm this hypothesis.

4.0 Conclusion/ Summary

In this report, a vanadium-based alloy was down-selected as candidates for fusion materials. The vanadium-based alloy material system was fabricated and processed to produce specimens with nanocrystalline, polycrystalline, and coarse grain sizes. Each condition was subjected to dual beam ion irradiation of 1 MeV Kr^{+} and 16 KeV He^{+} at the Intermediate Voltage Electron Microscope facility at Argonne National Laboratory. Results show that with finer grains, vanadium-based alloy demonstrates little grain coarsening even at temperatures as high as 700°C and possess promising radiation tolerance with the homogeneous distribution of He bubbles throughout the specimen. However, as the grain size grows larger, He bubbles begin to be observed and propagate at the grain boundaries. These suggest that for improved radiation tolerance, nanocrystallinity is critical.

5.0 References

[1] S.J. Zinkle, L.L. Snead, Designing radiation resistance in materials for fusion energy, Annual Review of Materials Research 44 (2014) 241-267.
[2] S.J. Zinkle, G. Was, Materials challenges in nuclear energy, Acta Materialia 61(3) (2013) 735-758.
[3] V. Philipps, Tungsten as material for plasma-facing components in fusion devices, J. Nucl. Mater. 415(1) (2011) S2-S9.
[4] J. Knaster, A. Moeslang, T. Muroga, Materials research for fusion, Nature Physics 12(5) (2016) 424-434.
[5] S. Kajita, W. Sakaguchi, N. Ohno, N. Yoshida, T. Saeki, Formation process of tungsten nanostructure by the exposure to helium plasma under fusion relevant plasma conditions, Nuclear Fusion 49(9) (2009) 095005.
[6] O. El-Atwani, J. Hinks, G. Greaves, S. Gonderman, T. Qiu, M. Efe, J.P. Allain, In-situ TEM observation of the response of ultrafine-and nanocrystalline-grained tungsten to extreme irradiation environments, Scientific reports 4 (2014) 4716.
[7] V. Sikka, J. Moteff, “Rafting” in neutron irradiated tungsten, Journal of Nuclear Materials 46(2) (1973) 217-219.
[8] O. El-Atwani, E. Aydogan, E. Esquivel, M. Efe, Y. Wang, S. Maloy, Detailed transmission electron microscopy study on the mechanism of dislocation loop rafting in tungsten, Acta Materialia 147 (2018) 277-283.
[9] T. Chookajorn, H.A. Murdoch, C.A. Schuh, Design of stable nanocrystalline alloys, Science 337(6097) (2012) 951-954.
[10] O. El-Atwani, W. Cunningham, E. Esquivel, M. Li, J. Trelewicz, B. Uberuaga, S. Maloy, In-situ irradiation tolerance investigation of high strength ultrafine tungsten-titanium carbide alloy, Acta Materialia 164 (2019) 547-559.
[11] E.P. George, D. Raabe, R.O. Ritchie, High-entropy alloys, Nature Reviews Materials (2019) 1.
[12] M.-H. Tsai, J.-W. Yeh, High-entropy alloys: a critical review, Materials Research Letters 2(3) (2014) 107-123.
[13] J.-W. Yeh, Recent progress in high-entropy alloys, Annales de Chimie. Science des Materiaux (Paris) 31(6) (2006) 633-648.
[14] Y. Zou, H. Ma, R. Spolenak, Ultrastrong ductile and stable high-entropy alloys at small scales, Nature communications 6 (2015) 7748.
[15] O.N. Senkov, G. Wilks, J. Scott, D.B. Miracle, Mechanical properties of Nb25Mo25Ta25W25 and V20Nb20Mo20Ta20W20 refractory high entropy alloys, Intermetallics 19(5) (2011) 698-706.
[16] R. Ursula, The Calphad method and its role in material and process development, Tecnologia em metalurgia, materiais e mineracao 13(1) (2016) 3-15.
[17] S. Thermo-Calc, TCS High Entropy Alloys Database (TCHEA5), (2021).
[18] I. Phases, A. Systems, MOBHEA2 : TCS High Entropy Alloy Mobility Database, (2018) 1-2.

Pacific Northwest National Laboratory

902 Battelle Boulevard
P.O. Box 999
Richland, WA 99354

1-888-375-PNNL (7665)

www.pnnl.gov